

# Superionicity and Polymorphism in Calcium Fluoride at High Pressure

Claudio Cazorla<sup>1,\*</sup> and Daniel Errandonea<sup>2</sup>

<sup>1</sup>*School of Materials Science and Engineering, University of New South Wales, Sydney NSW 2052, Australia*

<sup>2</sup>*Departamento de Física Aplicada (ICMUV), Universitat de Valencia, 46100 Burjassot, Spain*

We present a combined experimental and computational first-principles study of the superionic and structural properties of  $\text{CaF}_2$  at high  $P - T$  conditions. We observe an anomalous superionic behavior in the low- $P$  fluorite phase that consists in a decrease of the *normal*  $\rightarrow$  *superionic* critical temperature with compression. This unexpected effect can be explained in terms of a  $P$ -induced softening of a zone-boundary  $X$  phonon which involves exclusively fluorine displacements. Also we find that superionic conductivity is absent in the high- $P$  cotunnite phase. Instead, superionicity develops in a new low-symmetry high- $T$  phase that we identify as monoclinic (space group  $P2_1/c$ ). We discuss the possibility of observing these intriguing phenomena in related isomorphous materials.

PACS numbers: 66.30.H-, 81.30.Dz, 62.50.-p, 45.10.-b

Alkali earth metal fluorides (i.e.,  $\text{AF}_2$  compounds with  $A = \text{Ca}, \text{Sr}$  and  $\text{Ba}$ ) blend a family of extraordinary materials which for more than six decades have seduced both fundamental and applied physicists. Due to their low refractive index, low dispersion and large broadband radiation transmittance,  $\text{AF}_2$  have been extensively exploited in optical devices [1, 2]. These are also promising candidates for solid-state electrolytes to be used in batteries, as their internal electric currents dwell on the motion of ions [3–7].  $\text{CaF}_2$  is an archetypal ionic conductor and the most representative of  $\text{AF}_2$  species. Under ambient conditions  $\text{CaF}_2$  crystallizes in the fluorite structure ( $\alpha$ , space group  $Fm\bar{3}m$ ) wherein Ca atoms are cubic coordinated to F atoms. In  $\alpha\text{-CaF}_2$  a strong increase of the ionic conductivity is observed as  $T$  is raised up to  $\sim 1400$  K [8–10]. At this point the mobility of the fluorine anions is comparable to that of a molten salt, while the melting temperature of the system lies  $\sim 300$  K higher [11, 12].

The accepted dominant effect behind the large ionic conductivity observed in  $\alpha\text{-CaF}_2$ , dubbed as “superionicity”, is the formation of point Frenkel pair defects (FPD) (i.e., simultaneous creation of  $\text{F}^-$  vacancies and interstitials) [4, 5]. Yet, superionicity requires of abundant and correlated anion displacements thereby the formation of FPD by itself appears to be insufficient to fully elucidate the atomic mechanisms underlying it [13–15]. Moreover, this singular transport phenomenon remains surprisingly unexplored at moderate and high compressions. Almost 40 years ago, Mirwald and Kennedy were the first (and to the best of our knowledge the only so far) to experimentally study the high  $P - T$  phase diagram of  $\text{CaF}_2$  [16]. By relying on static compression methods and differential thermal analysis, they reported a continuous reduction of the critical temperature for the  $\alpha \rightarrow \beta$  transition (where  $\beta$  stands for the superionic phase)  $T_s$  under compression. This interesting and apparently puzzling effect has been overlooked for decades, calling for a meticulous revision with presently improved experimental techniques. Upon a pressure of  $\sim 10$  GPa  $\text{CaF}_2$  transforms

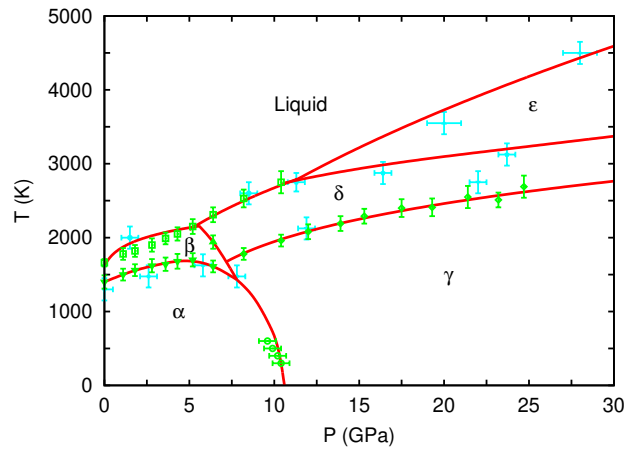


FIG. 1: (Color online) Proposed phase diagram of  $\text{CaF}_2$ . Greek letters represent normal ( $\alpha$ ,  $\gamma$  and  $\delta$ ) and superionic ( $\beta$  and  $\epsilon$ ) crystal phases, and the solid (red) lines their boundaries. Measurements and simulation results are indicated with open (green) and solid (blue) symbols, respectively.

into the orthorhombic cotunnite phase ( $\gamma$ , space group  $Pnma$ ), which can be structurally related to the cubic  $\alpha$ -phase through a local melting of the  $\text{F}^-$  sublattice [17]. The detailed ionic processes sustaining superionicity in this high- $P$   $\gamma$ -phase, however, are totally uncertain [18]. As for theory, only few simulation works have recently addressed the description of ionic conductivity at non-ambient conditions [19, 20]. Those few computational studies however rely all on molecular dynamics simulations performed with semi-empirical pairwise potentials which have been tuned to reproduce the behavior of  $\text{CaF}_2$  at ambient pressure. Whether the conclusions attained with those models at high  $P - T$  conditions may still be regarded as reliable, is an issue that needs to be clarified.

In this Letter, we present a combined experimental and first-principles computational study of the superionic and structural properties of  $\text{CaF}_2$  at high- $P$  and high- $T$ . Our observations and simulations disclose an anomalous su-

perionic behavior in  $\alpha$ -CaF<sub>2</sub> which consists of a decrease of  $T_s$  in the pressure interval  $5 \leq P \leq 8$  GPa. We find that such an anomaly can be caused by a  $P$ -induced softening of a zone-boundary  $X$  phonon, neither observed in SrF<sub>2</sub> nor in BaF<sub>2</sub>. Regarding  $\gamma$ -CaF<sub>2</sub>, our first-principles simulations show that large ionic conductivity is missing on this phase. Rather, superionicity appears after the crystal transforms via a second-order transition to a new low-symmetry high- $T$  phase that we identify as monoclinic (space group  $P2_1/c$ ).

We carried out two sets of experiments in CaF<sub>2</sub> [water-free 99.9 % purity (Sigma-Aldrich)] using a diamond-anvil cell (DAC). In the first set, Raman measurements were performed to determine the  $\alpha - \gamma$  phase boundary [21]. In these experiments, a 514.5 nm Ar<sup>+</sup> laser was used for Raman excitation and silicone-oil as a pressure transmitting medium. The temperature was fixed using an electric heating sleeve which surrounds the DAC body, and was measured using a K-type thermocouple [22]. The R<sub>1</sub> photoluminescence line of ruby and the <sup>7</sup>D<sub>0</sub>-<sup>5</sup>F<sub>0</sub> fluorescence of SrB<sub>4</sub>O<sub>7</sub>:Sm<sup>2+</sup> were used to determine  $P$  [23, 24]. In the second set of experiments, CaF<sub>2</sub> acted as the pressure medium and it was heated using the laser-heating technique. A tungsten (W) foil embedded in CaF<sub>2</sub> was heated with a Nd:YLF laser. The sample does neither absorb the laser radiation nor emit incandescent light in detectable amounts throughout all the studied  $P$  range. Therefore, following previous studies on alkali halides [25],  $T$  was measured from the W surface. Structural changes and melting were detected by visual observation using the laser speckle technique and a 632.8 nm He-Ne laser [26, 27]. Temperatures were determined by fitting a Planck function to the thermal emission spectra of W. Series of at least four experiments were performed for each transition. The assigned transition temperature was the average of all the measurements, and the corresponding error the maximum absolute deviation. After each heating cycle the DAC was inspected to check that neither chemical nor oxidation reactions had occurred in the metal surfaces [28]. The highest conditions reached in our experiments were  $T \sim 25$  GPa and  $P \sim 2500$  K.

Our first-principles density functional theory (DFT) calculations were performed with the generalized gradient approximation to the exchange-correlation energy due to Perdew [29]. We used the “projector augmented wave” method to represent the ionic cores [30], and considered Ca’s 6*p*-2*s* and F’s 2*s*-5*p* electronic states as valence. Wave functions were represented in a plane-wave basis truncated at 500 eV. By using these parameters and dense  $\mathbf{k}$ -point grids for Brillouin zone integrations, we obtained enthalpies converged to within 3 meV per formula unit. In the geometry relaxations, we imposed a force tolerance of 0.01 eV·Å<sup>-1</sup>. The agreement between our zero-temperature DFT calculations and the experimental equation of state and Raman frequencies is fairly good (see [31]). Details of our one-phase and two-phase

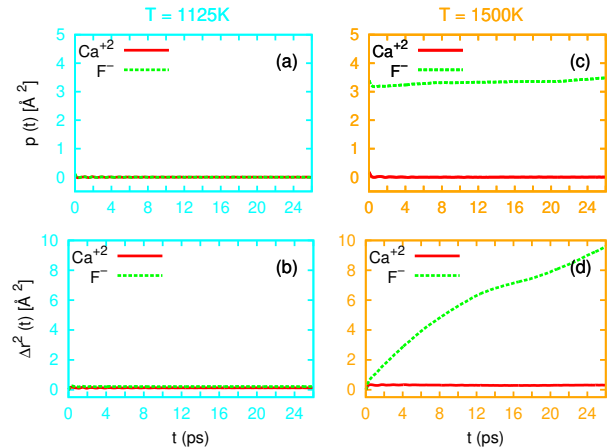


FIG. 2: Calculated position correlation function and mean squared displacement in CaF<sub>2</sub> at  $T = 1125$  K (a)-(b) and 1500 K (c)-(d) [ $P \sim 0$  GPa]. At 1500 (1125) K the system is in the  $\beta$  ( $\alpha$ ) phase [see text].

coexistence *ab initio* molecular dynamics (AIMD) simulations are explained in the Supporting Material [31].

In Fig. 1, we show the results of our DAC measurements and first-principles simulations in CaF<sub>2</sub>. As it can be appreciated, the agreement between experiments and calculations is remarkably good. Our results are also in accordance with previous data obtained by others at zero pressure [ $T_s = 1400(90)$  K and the melting temperature  $T_m = 1660(50)$  K] [8–12]. We attempted to estimate the  $\alpha - \gamma$  boundary by performing DFT free energy calculations within the quasi-harmonic approximation however, as we will explain later, this approach turns out to be inadequate for CaF<sub>2</sub>. The proposed CaF<sub>2</sub> phase diagram is very rich and complex: five different crystal phases [two of which are superionic ( $\beta$  and  $\epsilon$ ) and two unknown ( $\delta$  and  $\epsilon$ )] and four special three-fold coexistence points appear on it. Next, we concentrate on the two findings that we deem as the most relevant, namely (i) observation of anomalous superionic behavior in  $\alpha$ -CaF<sub>2</sub>, and (ii) appearance of two new high- $T$  phases ( $\delta$  and  $\epsilon$ ) one of which exhibits large ionic conductivity.

*Anomalous superionic behavior in  $\alpha$ -CaF<sub>2</sub>*—Slow motion of the speckle pattern under steady laser illumination was ascribed to the  $\alpha \rightarrow \beta$  transition (where  $\beta$  stands for the superionic state) in our experiments. The measured  $\alpha - \beta$  boundary displays a positive variation with increasing pressure at low  $P$ , reaching a maximum of  $T_s = 1700(90)$  at 5.2 GPa (in stark contrast to data reported by Mirwald and Kennedy [16]). At larger compressions, however,  $dT_s/dP$  unexpectedly becomes negative (see Fig. 1). This is in fact a very intriguing effect: if superionicity was uniquely mediated by Frenkel pair defects (FPD)  $T_s$  should necessarily increase with raising  $P$  because the formation energy of FPD escalates with compression (as we show in [31]). Indeed, other arguments

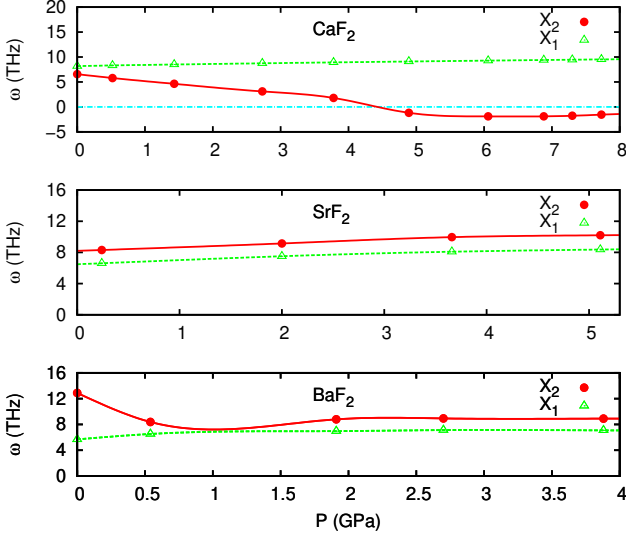


FIG. 3: Calculated frequencies of zone-boundary  $X$  phonon modes involving  $F^-$  displacements only, expressed as a function of pressure and  $AF_2$  species (cubic  $\alpha$  phase).

apart from FPD are needed to satisfactorily explain the observed  $T_s$  anomaly (and probably also superionicity).

In our AIMD simulations, we identified ionic conductivity by inspecting the calculated mean squared displacement  $\Delta r^2(t)$  of the  $Ca^{+2}$  and  $F^-$  ions [20]. To ascertain that the crystal remained vibrationally stable (i.e., the thermal average position of each ion remains centered on its perfect-lattice site), we computed the position correlation function  $p(t) \equiv \langle [\mathbf{r}_i(t+t_0) - \mathbf{R}_i^0] \cdot [\mathbf{r}_i(t_0) - \mathbf{R}_i^0] \rangle$  where  $\mathbf{r}_i(t)$  is the position of ion  $i$  at time  $t$ ,  $\mathbf{R}_i^0$  its perfect-lattice position,  $t_0$  an arbitrary time origin, and  $\langle \cdot \rangle$  denotes thermal average (see Fig. 2a-c) [32, 33]. The crystal is vibrationally stable if  $p(t \rightarrow \infty) = 0$  since the displacements at widely separated times become uncorrelated. On the contrary, if the atoms acquire a permanent vibrational displacement,  $p(t \rightarrow \infty)$  becomes non-zero. As it is shown in Fig. 1, the results obtained in our  $\alpha$ - $CaF_2$  simulations are in very good agreement with our DAC measurements: a negative  $dT_s/dP$  slope is found at pressures higher than  $\sim 5$  GPa. This remarkable agreement between theory and experiments certifies that the reported  $P$ -induced  $T_s$  anomaly constitutes a genuine effect. We note that none of the classical simulation works performed to date have reported any such peculiar behavior [19, 20], thus we may conclude that the employed interaction models are unsuitable to emulate  $CaF_2$  at high  $P - T$  conditions.

In the search to rationalize the origins of the observed  $T_s$  anomaly, we turned our attention onto collective phonon excitations [13–15]. Recently, an irregular  $T$ -dependence of a low-energy phonon mode at the  $X$  point of the Brillouin-zone boundary (single degenerate, labeled here as  $X_2$ ) has been observed in inelastic neutron

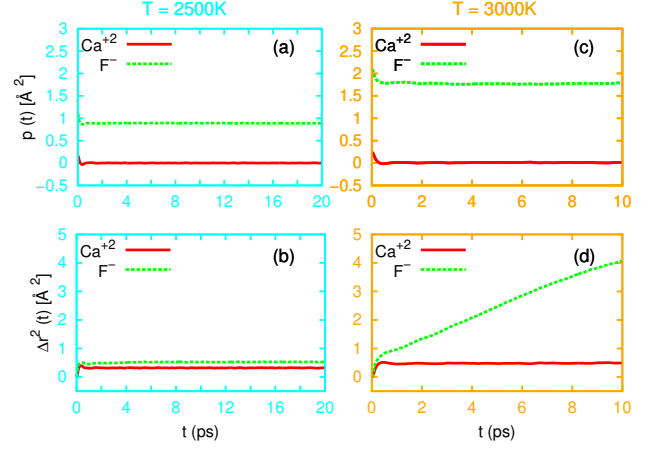


FIG. 4: Calculated position correlation function and mean squared displacement in  $CaF_2$  at  $T = 2500$  K (a)-(b) and  $3000$  K (c)-(d) [ $P \sim 17$  GPa]. At  $3000$  ( $2500$ ) K the system is in the  $\epsilon$  ( $\delta$ ) phase [see text].

scattering experiments [15]. That irregularity consists in a large decrease of its frequency with increasing temperature, which might be related to the onset of superionicity [13, 14, 34]. Motivated by these findings we studied the  $P$ -dependence of this and another zone-boundary  $X$  mode (doubly degenerate, labeled here as  $X_1$ ), both of which involve only the motion of  $F^-$  ions, with computational DFT methods (see Fig. 3) [31]. Our results show that the  $X_1$  frequency is always the highest and that it increases mildly with compression. The  $X_2$  mode, by contrast, softens significantly with pressure and its frequency eventually becomes imaginary at  $P \sim 4.5$  GPa. This predicted phonon mode softening marks the appearance of a collective instability within the  $F^-$  sublattice at a pressure that is similar to that identified with the  $T_s$  anomaly. In particular, the  $X_2$  eigenmode involves rows of anions moving anti-phase along an edge of their cubic lattice thus enhancing  $F^-$  disorder [13, 34]. We therefore link the causes behind the observed  $T_s$  anomaly with the predicted  $P$ -induced  $X_2$  mode softening in  $\alpha$ - $CaF_2$ . The results enclosed in Fig. 3 also show that standard quasi-harmonic approaches are inadequate to describe  $CaF_2$  under pressure because of the presence of imaginary phonon frequencies which are associated to large anharmonicity. Furthermore, aimed at disclosing whether the  $T_s$  anomaly could be observed also in other  $AF_2$  compounds, we carried out analogous phonon calculations in  $\alpha$ - $SrF_2$  and  $\alpha$ - $BaF_2$  (see Fig. 3). Our results show that both  $X_1$  and  $X_2$  zone-boundary modes behave normally on these materials, thus  $CaF_2$  appears to be unique of its kind.

*New high- $T$   $\delta$  and superionic  $\epsilon$  phases*— As  $\gamma$ - $CaF_2$  was stabilized in our DAC experiments and  $T$  increased steadily, we eventually observed a spatial fluctuation of the laser speckle that was markedly different from those

found in the previous analyzed transitions  $\alpha \rightarrow \beta$  and  $\beta \rightarrow \text{liquid}$ . Specifically, an intermittent laser speckle motion was detected that could be interpreted as a recrystallization process. In order to shed light on the nature of these observations, we performed new exhaustive AIMD simulations in  $\gamma$ -CaF<sub>2</sub>. The analysis of our computational results actually shows that the explained detections mark the occurrence of a continuous solid-solid transition (i.e., boundary  $\gamma - \delta$  in Fig. 1).

In Fig. 4a-b, we enclose the  $\Delta r^2$  and  $p$  functions obtained in CaF<sub>2</sub> at  $P \sim 17$  GPa and  $T = 2500$  K. The perfect-lattice positions entering function  $p$  are those of the cotunnite  $\gamma$  phase determined at zero temperature. The results in the figure reveal that at those conditions the diffusion of the F<sup>-</sup> anions is null while the cotunnite  $\gamma$  phase becomes vibrationally unstable [that is,  $\Delta r^2(t \rightarrow \infty) \sim \text{cte.}$  and  $p(t \rightarrow \infty) \neq 0$  for the F<sup>-</sup> anions]. In particular, the permanent displacements acquired by the fluorine anions suggest the happening of a continuous transformation from the cotunnite  $\gamma$  phase to a new unknown structure that we label as  $\delta$ . We repeated our simulations at different  $P - T$  conditions and arrived always at the same conclusions. Overall, our DFT estimations are in very good agreement with the series of measurements conforming the  $\gamma - \delta$  boundary (see Fig 1). By further raising  $T$  in our AIMD simulations, we found that large ionic conductivity appeared in the new high- $T$   $\delta$  phase (see Fig. 4c-d). This constitutes a very important finding since up to date it was assumed that superionicity in compressed CaF<sub>2</sub> appeared in the usual cotunnite  $\gamma$  phase [18]. We repeated our simulations at different  $P - T$  conditions and determined the entire  $\delta - \epsilon$  boundary, where  $\epsilon$  stands for the new high- $T$  superionic phase, up to  $\sim 25$  GPa (see Fig. 1). Meanwhile, none similar behavior to these just explained have been reported in any previous classical simulation work thus we reaffirm our conclusion that currently available CaF<sub>2</sub> interaction models are not adequate for high  $P - T$  analysis.

In our search to identify the symmetry of the newly discovered  $\delta$  phase, we initially turned our attention onto the hexagonal  $P6_3/mmc$  phase. We note that Dorfman *et al.* have recently reported a  $T$ -induced cotunnite to hexagonal phase transition in CaF<sub>2</sub> at pressures higher than  $\sim 60$  GPa [35] (see Fig. 5), hence the  $P6_3/mmc$  phase seems a natural candidate. However, after performing additional AIMD simulations we discarded this because the temperatures at which superionicity appeared were below the  $\delta - \epsilon$  boundary. Subsequently, we carried out intensive crystal searches in compressed CaF<sub>2</sub> based on diverse strategies, all which are detailed in the Supporting Material [31]. We found several structures which are energetically competitive with the  $\gamma$  phase at zero temperature, namely:  $P2_12_12_1$ ,  $Pmn2_1$ ,  $Pc$ ,  $P2_1$ , and  $P2_1/c$ . Of these candidates, we first chose the orthorhombic  $P2_12_12_1$  and  $Pmn2_1$ , and the monoclinic  $P2_1/c$  phases because a group-subgroup relationship ex-

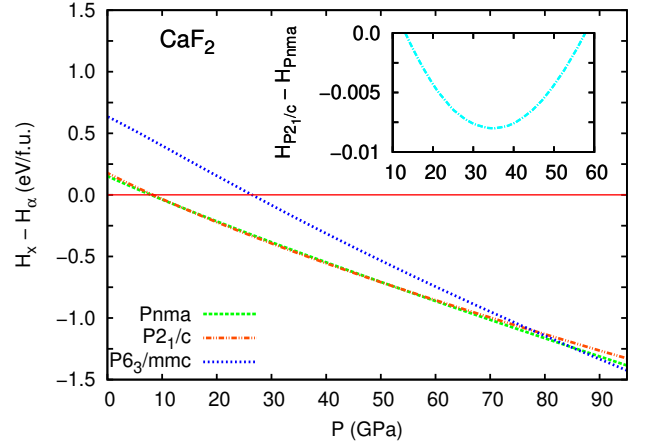


FIG. 5: Calculated enthalpy of several crystal structures referred to that of the cubic  $\alpha$  phase and expressed as a function of pressure. *Inset:* Detail of the enthalpy difference between the  $P2_1/c$  and  $Pnma$  phases.

ists between them and the orthorhombic  $\gamma$  phase (a condition that is required for a continuous phase transition [36, 37]). Finally, we concentrated in the monoclinic  $P2_1/c$  phase because this possessed the lowest energy. In Fig. 5, we plot the calculated enthalpy of this monoclinic phase in the  $0 \leq P \leq 100$  GPa interval and show that it strongly rivals that of the cotunnite structure (actually, at some points both enthalpy curves are indistinguishable within the numerical errors). We also computed its phonon spectrum at different pressures and found that it is mechanically and vibrationally stable (see [31]). Actually, the density of low-energy phonon modes in the monoclinic  $P2_1/c$  phase generally is slightly larger than in the orthorhombic  $Pnma$  phase, which is consistent with a possible  $T$ -induced phase transition between the two. As a conclusive test, we performed new exhaustive AIMD simulations in the  $P2_1/c$  phase and found that the calculated superionic temperatures were consistent with the  $\delta - \epsilon$  boundary previously determined. Based on these outcomes, we identify the new high- $T$   $\delta$  phase as monoclinic  $P2_1/c$ . This structure has a similar cation coordination polyhedra to that of the cotunnite phase: each Ca is linked to 9 fluorine atoms that form an elongated tricapped trigonal prism [31]. Furthermore, we performed enthalpy calculations also in SrF<sub>2</sub> and BaF<sub>2</sub> under pressure and found that the monoclinic  $P2_1/c$  phase is likewise energetically competitive in these materials (see [31]). Therefore, we may conclude that the  $\gamma \rightarrow \delta$  and  $\delta \rightarrow \epsilon$  transitions observed in CaF<sub>2</sub> are likely to happen also in SrF<sub>2</sub> and BaF<sub>2</sub>.

In summary, based on combined experimental DAC and first-principles simulation investigations we have characterized superionic conductivity in archetypal CaF<sub>2</sub> at high  $P - T$  conditions, and elucidated further the physical causes underlying it. Our findings are relevant also

to numerous compounds that are isomorphic to  $\text{CaF}_2$  including halides (e.g.,  $\text{PbCl}_2$ ), hydrides (e.g.,  $\text{CeH}_2$ ), nitrides (e.g.,  $\text{UN}_2$ ), and simple oxides (e.g.,  $\text{UO}_2$ ).

This work was supported under the Australian Research Council's Future Fellowship funding scheme (project number RG134363), and MICINN-Spain [Grants No. MAT2010-18113, No. CSD2007-00041, MAT2010-21270-C04-01, CSD2007-00045 and FIS2008-03845]. Computer resources, technical expertise and assistance were kindly provided by RES and CESGA. We acknowledge helpful comments from two of the referees on the proposed  $\text{CaF}_2$  phase diagram.

---

\* Electronic address: ccazorla@icmab.es; Corresponding Author

- [1] J. Barth, R. L. Johnson, M. Cardona, D. Fuchs, and A. M. Bradshaw, *Phys. Rev. B* **41**, 3291 (1990).
- [2] F. Gan, Y. N. Xu, Z. M. Huang, Y. W. Ching, and G. J. Harrison, *Phys. Rev. B* **45**, 8248 (1992).
- [3] W. Hayes and A. M. Stoneham in *Defects and Defect Processes in Non-metallic Solids*, (Wiley, New York 1985).
- [4] M. J. Gillan, *J. Phys. C* **19**, 3391 (1986); *J. Chem. Soc. Faraday Trans.* **86**, 1177 (1990).
- [5] P. J. D. Lindan and M. J. Gillan, *J. Phys.: Condens. Matter* **5**, 1019 (1993).
- [6] N. Sata, K. Eberman, K. Eberi, and J. Maier, *Nature (London)* **408**, 946 (2000).
- [7] C. S. Cucinotta, G. Miceli, P. Raiteri, M. Krack, T. D. Kühne, M. Bernasconi, and M. Parrinello, *Phys. Rev. Lett.* **103**, 125901 (2009).
- [8] C. E. Derrington, A. Lindner, and M. O'Keeffe, *J. Solid State Phys.* **15**, 171 (1975).
- [9] W. Hayes and M. T. Hutchings in *Ionic Solids at High Temperatures*, (World Scientific, Singapore 1985).
- [10] G. A. Evangelakis and V. Pontikis, *Europhys. Lett.* **8**, 599 (1989).
- [11] S. D. Mclaughlan, *Phys. Rev.* **160**, 287 (1967).
- [12] A. Mitchell and S. Joshi, *Metall. Trans.* **3**, 2306 (1972).
- [13] L. L. Boyer, *Phys. Rev. Lett.* **45**, 1858 (1980).
- [14] L. X. Zhou, J. R. Hardy, and H. Z. Cao, *Solid State Communications* **98**, 341 (1996).
- [15] K. Schmalzl, D. Strauch, and H. Schober, *Phys. Rev. B* **68**, 144301 (2003).
- [16] P. W. Mirwald and G. C. Kennedy, *J. Phys. Chem. Solids* **39**, 859 (1977).
- [17] S. E. Boulfelfel, *Phys. Rev. B* **74**, 094106 (2006).
- [18] S. Hull and D. A. Keen, *Phys. Rev. B* **58**, 14837 (1998).
- [19] Z.-Y. Zeng, X.-R. Chen, J. Zhu, and C.-E. Hu, *Chin. Phys. Lett.* **25**, 230 (2008).
- [20] C. Cazorla and D. Errandonea, *J. Phys. Chem. C* **117**, 11292 (2013).
- [21] S. Speziale and T.S. Duffy, *Phys. Chem. Minerals* **29**, 465 (2002).
- [22] D. Errandonea, D. Martínez-García, A. Segura, A. Chevy, G. Toblas, E. Canadell, and P. Ordejón, *Phys. Rev. B* **73**, 235202 (2006).
- [23] H. K. Mao, J. Xu, and P. Bell, *J. Geophys. Res.* **91**, 4673 (1986).
- [24] F. Datchi, R. Le Toullec, and P. Loubeyre, *J. Appl. Phys.* **81**, 3333 (1997).
- [25] R. Boehler, M. Ross, and D. B. Boercker, *Phys. Rev. B* **53**, 556 (1996).
- [26] D. Errandonea, R. Boehler, and M. Ross, *Phys. Rev. Lett.* **85**, 3444 (2000).
- [27] D. Errandonea, *Phys. Rev. B* **87**, 054108 (2013).
- [28] D. Errandonea, *J. Phys. Chem. Solids* **70**, 1117 (2009).
- [29] J. P. Perdew, K. Burke, and M. Ernzerhof, *Phys. Rev. Lett.* **77**, 3865 (1996).
- [30] P. E. Blöchl, *Phys. Rev. B* **50**, 17953 (1994).
- [31] See Supporting Material at xxx for more details of the DFT calculations, energy formation of FPD under pressure, zone-boundary  $X_2$  phonon mode, crystal structure searches, and the monoclinic  $P2_1/c$  phase.
- [32] C. Cazorla, D. Alfè, and M. J. Gillan, *Phys. Rev. B* **85**, 064113 (2012).
- [33] L. Vočadlo, D. Alfè, M. J. Gillan, I. G. Wood, J. P. Brodholt, and G. D. Price, *Nature (London)* **424**, 536 (2003).
- [34] L. L. Boyer, *Solid State Ionics* **5**, 581 (1981).
- [35] S. M. Dorfman, F. Jiang, Z. Mao, A. Kubo, Y. Meng, V. B. Prakapenka, and T. S. Duffy, *Phys. Rev. B* **81**, 174121 (2010).
- [36] H. T. Stokes and D. M. Hatch, *Phys. Rev. B* **30**, 4962 (1984).
- [37] S. Ivantchev, E. Kroumova, G. Madariaga, J. M. Pérez-Mato, and M. I. Aroyo, *J. Appl. Cryst.* **33**, 1190 (2000).